Analysis of Models for Determining Intestinal Wall Permeabilities

G. L. AMIDON *x, J. KOU *, R. L. ELLIOTT *, and E. N. LIGHTFOOT ‡

Received February 27, 1980, from the *School of Pharmacy and the ‡Department of Chemical Engineering, University of Wisconsin, Madison, WI 53706. Accepted for publication June 11, 1980.

Abstract □ In determining intestinal wall permeabilities, several mass transport models may be applied to analyze the results from external perfusion experiments. The appropriateness of any given model depends on the applicability of the model assumptions to the experimental system. This report compares several mass transport models with respect to their assumptions and applicability to a particular experimental design. The models are shown to differ in their assumptions regarding convection and diffusion in the perfusing fluid. However, since the wall permeability is an unknown parameter in each model and is estimated from the data, all of the models fit the mass transfer results reasonably well, despite fundamentally different assumptions. However, the determined permeabilities differ. Residence time distribution analysis of the experimental system is more sensitive to the model assumptions. It is shown that, in a particular experimental system, laminar flow in a cylindrical tube is the most appropriate model. The model also has the advantage of implicitly accounting for the convection–diffusion problem in the perfusing fluid. Hence, the diffusion layer thickness is not estimated from the data. With the hydrodynamics defined, the relative permeabilities resulting from the application of the several models to the data can be interpreted. The wall permeability determined in the suggested manner provides an estimate of the limiting assistance under perfect mixing conditions.

Keyphrases □ Permeability—mass transport models of intestinal wall permeability □ Models, hydrodynamic—mass transport models of intestinal wall permeability □ Diffusion—mass transport models of intestinal wall permeability

In determining the permeability of the intestinal wall by external perfusion techniques, several models have been proposed (1–5). In each model, assumptions must be made regarding the convection and diffusion conditions in the experimental system. These assumptions, in turn, affect the interpretation of the resulting permeabilities. In addition, the appropriateness of the assumptions in the models to the actual experimental situation must be determined. Often, good agreement between the predicted (theoretical) result and the experimental result is used to support the validity of the model. However, in many cases, several models may be equally satisfactory, particularly when significant variation occurs from experiment to experiment. In this situation, independent experiments that are more sensitive to the assumptions in the models are needed to substantiate their validity.

This report shows that several reasonable models for mass transfer in external perfusion experiments can account for the data reasonably well because the actual wall permeability is unknown. That is, if the permeability is treated as a parameter and is estimated from the data, all of the models can describe the data relatively well.

However, the resulting permeabilities differ, and their interpretation rests on the validity of the assumptions. Consequently, residence time distribution analysis is used to obtain more direct insight into the convection and diffusion assumptions of the mass transfer models. Since the laminar flow model discussed previously (5) has the advantage of providing a direct measure of the wall permeability, the experimental system used was one that maximizes the possible attainment of these conditions.

EXPERIMENTAL

[^{14}C]Polyethylene glycol[1] was used for the residence time studies. Assays were conducted by liquid scintillation. For the residence time perfusion experiments, male Holtzman rats (250–350 kg) were fasted for 12–18 hr and anesthetized with an intramuscular (gluteal muscle) dose of 150 mg/100 g with a 50% urethan solution. A midline abdominal incision was made, and the intestine was cannulated 2 and 10 cm distal to the ligament of Treitz. The entrance tubing was connected to a three-way stopcock such that the test solution would flow straight through the stopcock. The buffer solution, isotonic Sorensen's buffer at pH 7.3, was perfused through the remaining stopcock arm for 20–30 min.

The experiment was initiated by turning the stopcock to the test solution (polyethylene glycol–Sorensen's buffer) at time zero. Samples were collected at 15-sec intervals for ~2 min ($2\bar{t}$) and then at 30-sec intervals for up to ~6 min ($6\bar{t}$). From the collected samples, 0.1 ml was transferred by micropipet to the counting vial. For the step change in concentration, the test solution was perfused throughout the experiment. For the (finite) pulse change, the stopcock was switched from the buffer to the test solution and back to the buffer over about a 2-sec interval. The flow rate was 0.5 ml/min for all experiments.

At the conclusion of the experiment, the animal was sacrificed and the cannulated intestine was excised. The length and volume of the excised intestine were measured to estimate the residence time in the perfused segment. The mass transfer studies used [^{3}H]estrone[1] and followed a procedure described previously (6).

RESULTS AND DISCUSSION

Mass Transfer Models—Four models will be described that differ in their convection and diffusion assumptions (Fig. 1). These models include the laminar flow, plug flow, and complete radial mixing (diffusion layer) models for convective mass transport in a tube and the perfect mixing tank model. It is convenient to begin with the solute transport equation in cylindrical coordinates (5, 7):

$$v_z \frac{\partial C}{\partial z} = D \frac{1}{r} \frac{\partial}{\partial r}\left(r \frac{\partial C}{\partial r}\right) \qquad \text{(Eq. 1)}$$

where:

v_z = axial velocity distribution
D = solute diffusivity in the solvent
C = concentration of A in B
z = axial coordinate
r = radial coordinate

Introduction of the dimensionless variables:

$z^* = z/L$
$r^* = r/R$
$v_z^* = v_z/V_m$
$Gz = DL/V_mR^2 = \pi DL/2Q$
R = radius of the tube
L = length of the tube
V_m = maximum velocity
Q = perfusion flow rate

gives:

[1] New England Nuclear, Boston, Mass.

0022-3549/80/1200-1369$01.00/0

Table I—Summary of Various Models

Model	Equation	Variables	Comments
Laminar flow	$C_m/C_0 = \Sigma M_n \exp(-\beta_n^2 Gz)$	P_w^* and Gz	M_n and β_n are functions of P_w^* (Ref. 5)
Plug flow	$C_m/C_0 = \Sigma M'_n \exp(-\beta_n'^2 Gz)$	$P_w'^*$ and Gz	M'_n and β'_n are functions of $P_w'^*$ (Ref. 8)
Complete radial mixing	$C_m/C_0 = \exp(-4P_{eff}^* Gz)$	P_{eff}^* and Gz	$P_{eff}^* = \frac{P_a^* P_w^*}{P_a^* + P_w^*}$
Mixing tank	$C_m/C_0 = (1 + 4P_{eff}'^* Gz)^{-1}$	$P_{eff}'^*$ and Gz	$P_{eff}'^* = \frac{P_a'^* P_w^*}{P_a'^* + P_w^*}$

$$v_z^* \frac{\partial C}{\partial z^*} = Gz \left(\frac{1}{r^*} \frac{\partial}{\partial r^*} r^* \frac{\partial C}{\partial r^*} \right) \quad \text{(Eq. 2)}$$

This relationship is subject to the first-order boundary condition at the wall:

$$\left. \frac{\partial C}{\partial r^*} \right|_{r^*=1} = -P_w^* C_w \quad \text{(Eq. 3)}$$

where $P_w^* = P_w R/D$ = the dimensionless wall permeability.

The main assumptions in arriving at Eqs. 1 and 2 are: (*a*) the diffusivity and density are constant; (*b*) the solution is dilute so that the solvent convection is unperturbed by the solute; (*c*) the system is at steady state ($\partial C/\partial t = 0$); (*d*) the solvent flows only in the axial (z) direction; (*e*) the tube radius, R, is independent of Gz; and (*f*) axial diffusion is small compared to axial convection (7). The boundary condition (Eq. 3) is true for many models having a tube wall but does not describe a carrier transport or Michaelis–Menten process at the wall, except at low solute concentrations. Rewriting Eqs. 2 and 3[2] gives:

$$v_z^* \frac{\partial C}{\partial z} = Gz \left(\frac{1}{r} \frac{\partial}{\partial r} r \frac{\partial C}{\partial r} \right) \quad \text{(Eq. 4)}$$

$$\left. \frac{\partial C}{\partial r} \right|_{r=1} = -P_w^* C_w \quad \text{(Eq. 5)}$$

It is clear that the solution is $C = C(r, z, Gz, P_w^*)$. That is, Gz and P_w^* are the two fundamental independent (dimensionless) variables. Since the measured exit concentration is generally a velocity-averaged concentration (cup-mixing concentration), averaging over r gives:

$$C_m(Gz, P_w^*) = \frac{\int_0^{2\pi} \int_0^1 v_z C r \, dr \, d\theta}{\int_0^{2\pi} \int_0^1 v_z r \, dr \, d\theta} \quad \text{(Eq. 6)}$$

where z (dimensionless) is set equal to 1 (*i.e.*, the concentration is measured at the end of the tube). For the several models discussed here, the given solution refers to the cup-mixing concentration, and Gz and P_w^* are the only fundamental independent variables. However, the P_w^* value will have different interpretations within the context of the different models.

Laminar Flow Model—In the laminar flow model, the velocity profile is taken to be that for a Newtonian fluid in a tube:

$$v_z^* = v_z/V_m = 1 - r^2 \quad \text{(Eq. 7)}$$

where $V_m = 2\langle v \rangle$ and $\langle v \rangle$ is the average flow velocity; *i.e.*, $Q = \langle v \rangle \pi R^2$. With this velocity profile, Eq. 4 is separable and with the boundary condition in Eq. 5 has the solution (5):

$$C_m/C_0 = \sum_n M_n \exp(-\beta_n^2 Gz) \quad \text{(Eq. 8)}$$

where C_m is the exit cup-mixing concentration at length L and C_0 is the inlet concentration (constant). The laminar flow model will be discussed in detail in a report[3] that also contains tabulated values of the M_n and β_n values as a function of P_w^*.

Plug Flow Model—In the plug flow model, the velocity profile is considered to be independent of both r and z. That is, $v_z = Q/\pi R^2$ and is constant; hence, $V_z = V_m$ and $V_z^* = 1$. The solution to Eqs. 4 and 5 is (8):

$$C_m/C_0 = \Sigma M'_n \exp(-\beta_n'^2 Gz) \quad \text{(Eq. 9)}$$

where $M'_n = -4P_w'^*/(\beta_n'^4 + \beta_n'^2 P_w'^{*2})$ and the β'_n values are the roots of the equation:

$$\beta' J_1(\beta') - P_w'^* J_0(\beta) = 0 \quad \text{(Eq. 10)}$$

with J_1 and J_0 being zero-order bessel functions of the first and second kinds. The roots of Eq. 10 are tabulated in Refs. 8 and 9.

With this model, the assumption that V_z is constant is one of perfect slip at the wall. That is, V_z is constant throughout the fluid while the velocity of the wall is zero. However, there is radial diffusion as well as a corresponding concentration gradient toward the wall. The $P_w'^*$ value is the true wall permeability if the actual hydrodynamics are of this type. For a given wall permeability, the plug flow model predicts greater absorption of the solute compared to the laminar flow model due to greater convection near the wall.

Complete Radial Mixing Model—For this model, the velocity profile is assumed to be constant as with the plug flow model. In addition, the concentration is assumed to be constant radially but not axially. That is, there is complete radial, but not axial, mixing to give uniform radial velocity and concentration profiles. With these assumptions, Eq. 4 and

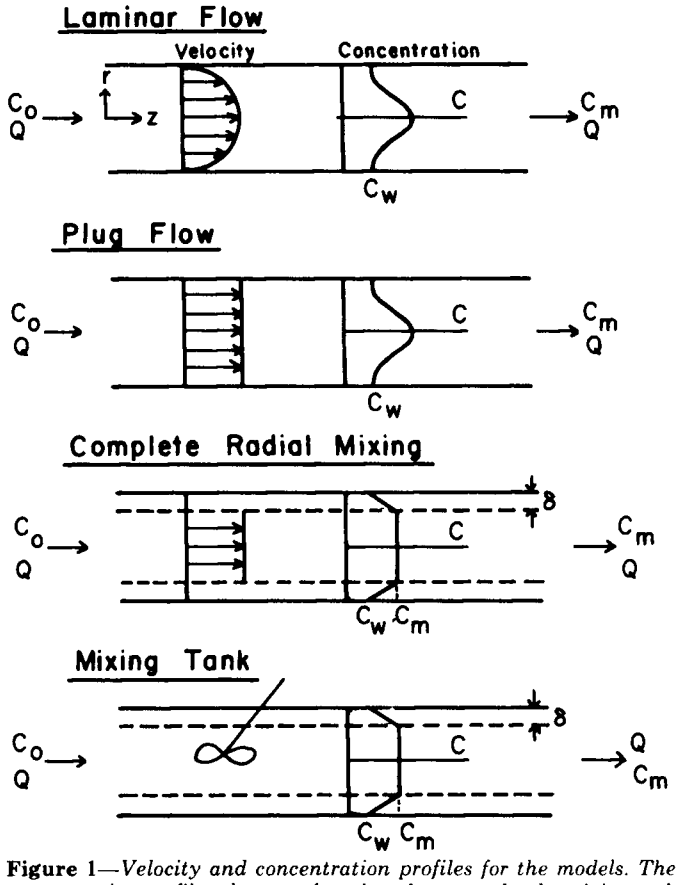

Figure 1—*Velocity and concentration profiles for the models. The concentration profiles also are a function of z except for the mixing tank model.*

[2] Hereafter, all equations will be in dimensionless form but the asterisk will be deleted from the r and z symbols except where the context clearly indicated otherwise.

[3] See R. L. Elliott, G. L. Amidon, and E. N. Lightfoot, *J. Theor. Biol.*, in press.

the boundary condition (Eq. 5) have the solution (5):

$$C_m/C_0 = \exp(-4P^*_{eff}Gz) \quad \text{(Eq. 11)}$$

where P^*_{eff} replaces P^*_w. Since no aqueous resistance is included directly in the model, the wall resistance usually is augmented with a film or diffusion layer resistance. That is, complete radial mixing occurs up to a thin region or film adjacent to the membrane. The aqueous (luminal) resistance is confined, within this model, entirely to this region in series with the membrane. Hence, the wall permeability includes an aqueous or luminal resistance term and can be written as:

$$P^*_{eff} = \frac{P^*_w P^*_a}{P^*_w + P^*_a} \quad \text{(Eq. 12)}$$

where P^*_w is the true wall permeability and P^*_a is the effective aqueous permeability (1–3, 5).

The aqueous permeability often is written as:

$$P_a = D/\delta \quad \text{(Eq. 13)}$$

or:

$$P^*_a = R/\delta \quad \text{(Eq. 14)}$$

where δ is the film thickness and represents an additional parameter that needs to be determined from the data to obtain P^*_w. Since the assumed hydrodynamic conditions probably are not realistic at the low Reynolds numbers for typical experiments, P^*_a or δ/R is an empirical parameter.

The complete radial mixing model also can be derived from a differential mass balance approach (1) and often is referred to as the diffusion layer model. A comparison of the laminar flow and complete radial mixing models will be reported later[3].

Mixing Tank Model—This model takes the next step and assumes that both radial and axial mixing are complete. The aqueous resistance again is thought to be confined to a region (film) next to the membrane where only molecular diffusion occurs, whereas the rest of the contents are well mixed (perfect mixer). This model is described most easily by a mass balance on the system:

$$(\text{mass/time})_{inlet} - (\text{mass/time})_{outlet} = (\text{mass/time})_{absorbed} \quad \text{(Eq. 15a)}$$

or:

$$QC_0 - QC_m = (2\pi RL)(P'_{eff})C_m \quad \text{(Eq. 15b)}$$

where $2\pi RL$ is the area of the mass transfer surface (cylinder) of length L and radius R, P'_{eff} is the permeability or mass transfer coefficient of the surface, and C_m is the concentration in the tube (which is constant and equal to the outlet concentration by the perfect mixing assumption). From Eq. 15b is obtained:

$$\frac{C_0 - C_m}{C_m} = P'_{eff}\frac{2\pi RL}{Q} \quad \text{(Eq. 16)}$$

or:

$$C_0/C_m = 1 + 4P'^*_{eff}Gz \quad \text{(Eq. 17)}$$

As with the complete radial mixing model, P'^*_{eff} contains the additional parameter $P'^*_a = R/\delta'$ that must be estimated from the data. The P'^*_a and P'^*_{eff} values for the mixing tank model differ from those for the complete radial mixing model by nature of the different hydrodynamic assumptions. While this model probably is not appropriate to most perfusion experiments, it will be useful to compare its ability to correlate mass transfer data with the other models.

Model Comparison and Summary—Table I summarizes the models with respect to the predicted mass transfer. If the true wall permeability, P^*_w, were known, then each model could be tested against the data to determine its ability to reproduce the data. Since this is not the case, the appropriate P^*_w or P^*_{eff} value must be determined from the data. A test of the model then is to determine its ability to correlate the data, given a value for the permeability (estimated from the data). That is, the equations in Table I correlate the observed C_m/C_0 as a function of the Gz value, with the permeability being used as a variable parameter.

Mass Transfer Results—Figure 2 presents the results using the simple mixing tank model (Eq. 17). The best-fit line (with zero intercept) is:

$$(C_0/C_m) - 1 = 6.97Gz \quad \text{(Eq. 18)}$$

with $n = 17$, $s = 0.064$, and $p < 0.0005$. The standard error of the slope is 0.43. The P'^*_{eff} calculated from Eq. 17 is 1.7. Given the simplicity of the model, it accounts for the data reasonably well. However, from the graph, it is clear that systematic deviations occur from the best-fit line. If the two data points at the highest Gz value were removed from the data set, the model would do quite well.

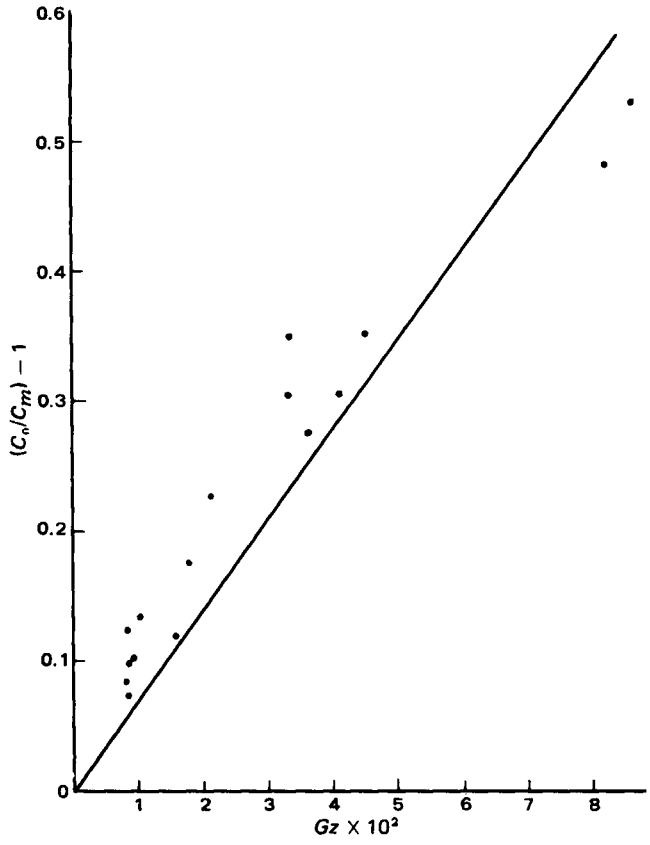

Figure 2—*Graph of* $(C_0/C_m) - 1$ versus Gz *following the mixing tank model* (—) *and the experimental data* (●) *for estrone.*

Figure 3 presents the data as well as the best-fit lines for all four models. The permeabilities were estimated *via* linear regression following Eqs. 11 and 17 and by nonlinear regression following Eqs. 8 and 9 for the respective models. The resulting permeabilities are given in Table II. From Fig. 3, it is clear that it is not possible to choose from among the models on the basis of the mass transfer data if the permeability itself is estimated from the data. The permeabilities differ for the various models. Interpretation of the respective permeabilities requires knowledge as to which model most closely reflects the actual experimental situation.

Residence Time Distribution Analysis—To interpret the mass transfer results and the associated permeabilities, it is necessary to establish the actual hydrodynamics. Since, as noted, the mass transfer data are not sensitive to the model if the wall permeability is known, an independent method that is more sensitive to the hydrodynamics is required. In any given situation, the hydrodynamics implied (assumed) by one or another of the mass transfer models may be the most appropriate. The experimental design used for this study maximized the possible attainment of laminar flow.

Residence time distribution analysis provides one method for determining flow characteristics (10–12). A step or pulse change in the inlet concentration of a completely inert tracer is made, and the resulting appearance of the tracer in the outlet stream is monitored. The appear-

Table II—Permeability Values Estimated from the Data for the Various Models

Model	Permeability[a]
Mixing tank	1.7 (±0.9)
Complete radial mixing	2.0 (±0.3)
Plug flow	3.1 (±0.5)
Laminar flow	5.7 (±1.3)

[a] Dimensionless permeability. Values in parentheses represent the approximate 95% confidence intervals.

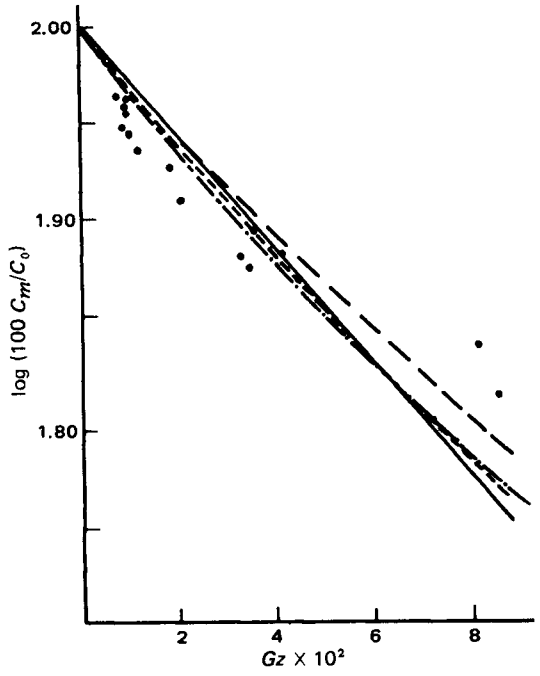

Figure 3—*Graph of log(100*C_m/C_0*) versus Gz for the several models and the experimental data (●) for estrone. Key: – –, mixing tank model; —, complete radial mixing model; - - -, plug flow model; and · – ·, laminar flow model.*

ance of tracer in the outlet stream is a function of the flow (hydrodynamic) conditions since these conditions, in turn, determine the length of time a given fluid element entering the inlet stays in the apparatus. In dealing with potentially very simple hydrodynamics, three simple models are appropriate: mixing tank, plug flow, and laminar tube flow. The step change in concentration, $C = 0$ at $t < 0$ and $C = C_0$ at $t > t_0$, at the inlet gives the F curve, while a finite pulse change (12) gives the E curve. The F curve is defined as:

$$F = \langle C \rangle / C_0 \qquad \text{(Eq. 19)}$$

where $\langle C \rangle$ is the exit cup-mixing concentration and C_0 is the inlet concentration.

The E curve is defined by:

$$E = dF/dt \qquad \text{(Eq. 20)}$$

For a pulse change in concentration at the inlet with a total mass, M, of tracer injected:

$$M = \int_0^\infty \langle C \rangle \, dt \qquad \text{(Eq. 21)}$$

and the E curve is obtained from:

$$E = \frac{\langle C \rangle}{M} \qquad \text{(Eq. 22)}$$

The (experimental) mean residence time, $\bar{t}$, in the apparatus is obtained from:

$$\bar{t} = \int_0^\infty \bar{t} E \, dt \qquad \text{(Eq. 23)}$$

for the pulse change and from:

$$\bar{t} = \int_0^\infty (1 - F) \, dt \qquad \text{(Eq. 24)}$$

for the step change. The corresponding F and E functions for the plug flow model are:

$$F = 0 \qquad t < \bar{t} \qquad \text{(Eq. 25a)}$$

$$F = 1 \qquad t > \bar{t} \qquad \text{(Eq. 25b)}$$

$$E = 0 \qquad t \neq \bar{t} \qquad \text{(Eq. 25c)}$$

$$E = \text{input function} \qquad t = \bar{t} \qquad \text{(Eq. 25d)}$$

For the perfect mixer model, they are:

$$F = 1 - e^{-t/\bar{t}} \qquad \text{(Eq. 26a)}$$

$$E = \frac{1}{\bar{t}} e^{-t/\bar{t}} \qquad \text{(Eq. 26b)}$$

For the laminar flow model, they are:

$$F = 1 - \left(\frac{\bar{t}}{2t}\right)^2 \qquad t > \bar{t}/2 \qquad \text{(Eq. 27a)}$$

$$E = \frac{\bar{t}^2}{2} \frac{1}{t^3} \qquad t > \bar{t}/2 \qquad \text{(Eq. 27b)}$$

The theoretical E and F curves for these models using $\theta = t/\bar{t}$ as dimensionless time are shown in Fig. 4. These models contain only one parameter, $\bar{t}$.

More complex, two- (or more) parameter models, *e.g.*, tanks in series or a dispersion model, could be fitted to the data. However, given the simplicity of the flow situation, this is unnecessary.

The experimental results from the intestinal perfusion studies also are shown in Fig. 4. Since the plug flow model clearly is inappropriate, it will not be analyzed further.

Table III presents the mean residence times estimated by the following three methods: (*a*) the volume measurement of the intestine at $\bar{t} = V/Q$,

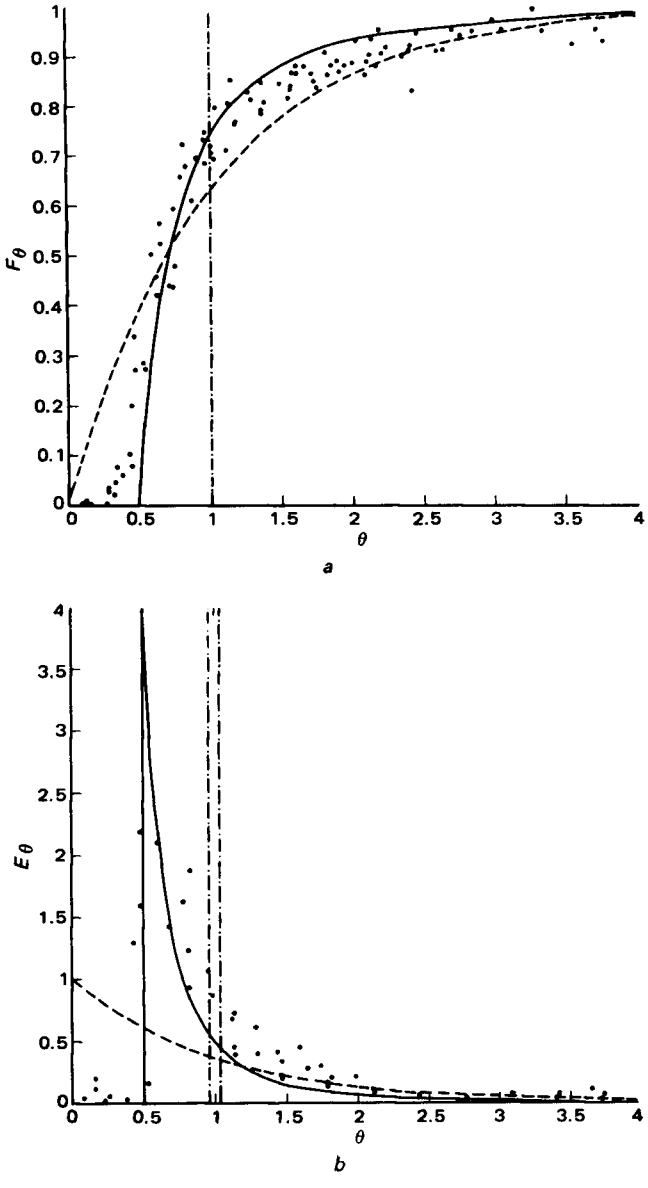

Figure 4—*Curves for perfusion experiments,* F versus θ = t/$\bar{t}$ (a) *and* E versus θ (b). *Key: - - -, mixing tank model; —, laminar flow model; - · -, plug flow model; and ●, experimental results.*

Table III—Estimated Mean Residence Times

Experiment[a]	$\bar{t}\left(\frac{V}{Q}\right)$	$\bar{t}$ (Area)	Mixing Tank $\bar{t}$ (regression)[b]	Laminar Flow $\bar{t}$ (regression)[b]
1	65	60.6	63.9 (13)	60.8 (5)
2	65	51.5	52.4 (8)	57.8 (5)
3	65	52.6	53.0 (11)	56.8 (4)
4	97	70.1	67.5 (13)	76.1 (9)
5	97	86.2	82.7 (23)	79.4 (5)
6	97	82.3	74.8 (11)	77.2 (13)
7	78	65.5	55.8 (11)	55.7 (5)
8	78	71.5	68.7 (16)	65.0 (2)
9	78	81.2	75.8 (14)	76.2 (10)
10	43	46.0	73.6 (75)	37.4 (2)
11	43	46.2	70.6 (63)	34.6 (3)
12	85	86.6	230.3 (300)	89.9 (8)
13	85	99.2	237.0 (310)	74.9 (1)

[a] Experiments 1–9 represent step changes in inlet concentration, and Experiments 10–13 represent pulse changes in concentration. [b] Numbers in parentheses represent approximate 95% confidence intervals.

(*b*) integration following Eq. 23 or 24, and (*c*) nonlinear regression fitting of the mixing tank and laminar flow models to the data using the mean residence time, $\bar{t}$, as the only parameter.

The results in Fig. 4 and Table II clearly suggest that the laminar flow model is the most appropriate of the three simple models. However, the data suggest that some mixing or dispersion is occurring in the system since the tracer appears at the outlet somewhat faster than laminar flow would predict.

Interpretation of Mass Transfer Data—Given the results of the residence time studies, the permeabilities are interpreted most appropriately on the basis of laminar flow hydrodynamics. The estrone permeability value of 6, determined under the assumption of laminar flow, represents an estimate of the true wall permeability. The luminal diffusive component, P^*_{aq}, is not included in the wall permeability. In fact, if the flow is laminar, P^*_{aq} can be calculated from the model (5).

Assuming that the laminar flow permeability measures the wall permeability, the permeabilities resulting from application of the other models can be interpreted. The plug flow value of 3 is lower than the laminar flow result since a larger membrane resistance is needed to compensate for the lower estimate of the aqueous resistance. That is, the larger amount of convection near the wall in the plug flow model leads to a larger P^*_{aq} than actually is the case. Consequently, the membrane permeability must be lower to account for the observed result.

The permeability value for the complete radial mixing model of 2 is lower than the plug flow (and laminar flow) model since this model assumes radial mixing, which leads to still lower estimated luminal (aqueous) resistance values and a higher estimated membrane resistance (lower permeability value). However, the usual interpretation of the complete radial mixing model recognizes that the permeability value includes an aqueous (film) resistance.

The mixing tank model takes the final step in assuming both radial and axial mixing. The permeability value for this model is the lowest of all of the models. Again, this result is due to the low luminal resistance implied by the model. As with the complete radial mixing model, a film resistance usually is included in the wall permeability to account for the presence of an aqueous resistance.

If, as suggested, the complete radial mixing permeability includes a film (diffusion layer) aqueous resistance, the permeability value should be that obtained from the laminar flow model augmented by a P^*_{aq} value following Eq. 12. However, P^*_{aq} is a function of both P^*_w and Gz and, hence, must be calculated at every flow rate (Gz value) using the known P^*_w value. However, an estimate of P^*_{aq} can be made that is not greatly in error by using the ${}^0P^*_{aq}$ value for sink conditions at the wall and an average Gz value (5). This approach gives ${}^0P^*_{aq} = 3.7$. The predicted permeability for the complete radial mixing model thus is 2.2, which is in good agreement with the estimated value of 2.0. A more detailed discussion of the basis for this calculation was given previously (5, 6).

This discussion illustrates one major advantage of the laminar flow approach. The diffusion layer thickness is not a parameter in the model, and the wall permeability can be calculated directly. In the complete radial mixing model, the P^*_{aq} (equal to R/δ) value enters the model to account for the unknown hydrodynamics and, hence, must be estimated from the data as well. The residence time distribution analysis indicates that laminar flow can be established to a reasonable approximation in external perfusion experiments. Consequently, there is no need to introduce a new parameter.

With respect to the normal physiological situation, the hydrodynamics clearly are much more complex. However, the wall permeability is of intrinsic interest since it represents the limiting (controlling) resistance under perfect mixing conditions. Consequently, the wall permeability can be used to quantitate the absorption characteristics of drugs as well as for an experimental approach to the study of the nature of the wall resistance.

CONCLUSION

Four mass transport models that can be applied to intestinal perfusion studies were developed and compared. The models differ with respect to the assumptions regarding convection and diffusion in the perfusing fluid. If the wall permeability is estimated from the experimental results, all of the models work reasonably well. The wall permeabilities fall in the order mixing tank < complete radial mixing (diffusion layer) < plug flow < laminar flow.

Residence time distribution analysis was employed as a more sensitive measure of the validity of the underlying model assumptions. In the experimental system employed, laminar flow in a circular duct is the most appropriate model. This model provides the most direct measure of the intrinsic wall (membrane) permeability. The permeabilities for the various models are in the expected order for the test system, with the wall permeability decreasing in direct proportion to the extent to which the models overestimate the aqueous permeability.

It is concluded that laminar flow in an externally perfused intestine is attainable experimentally and provides the most direct measure of the intrinsic wall permeability. The wall permeability, in turn, represents the limiting permeability under perfect mixing conditions.

REFERENCES

(1) N. F. H. Ho and W. I. Higuchi, *J. Pharm. Sci.*, **63**, 686 (1974).

(2) J. M. Dietschy and H. Westergaard, in "Intestinal Absorption and Malabsorption," T. Z. Csaky, Ed., Raven, New York, N.Y., 1975, p. 197.

(3) D. Winne, *Arch. Pharmacol.*, **304**, 175 (1978).

(4) *Ibid.*, **307**, 265 (1979).

(5) R. L. Elliott, Ph.D. thesis, University of Wisconsin, Madison, Wis., 1979.

(6) G. L. Amidon, G. D. Leesman, and R. L. Elliott, *J. Pharm. Sci.*, **69**, 1363 (1980).

(7) R. B. Bird, W. E. Stewart, and E. N. Lightfoot, "Transport Phenomena," Wiley, New York, N.Y., 1960, p. 559.

(8) H. S. Carslaw and J. C. Jaeger, "Conduction of Heat in Solids," 2nd ed., Oxford University Press, Oxford, England, 1959, p. 195.

(9) M. Abramowitz and I. A. Stegun, "Handbook of Mathematical Functions," Dover, New York, N.Y., 1972, p. 414.

(10) O. Levenspiel, "Chemical Reaction Engineering," 2nd ed., Wiley, New York, N.Y., 1972, p. 253.

(11) C. G. Hill, "An Introduction to Chemical Engineering Kinetics and Reactor Design," Wiley, New York, N.Y., 1977, p. 388.

(12) C. Y. Wen and L. T. Fan, "Models for Flow Systems and Chemical Reactors," Dekker, New York, N.Y., 1975.

ACKNOWLEDGMENTS

Supported by the University of Wisconsin Graduate School, The Upjohn Company, Biomedical Research Support Grant SO 7RR05456-17, and GM 27680.